Nigerian Journal of Technology (NIJOTECH)
Vol. 45 No. 2 June 2026 pp. 307-319
www.nijotech.com

Print ISSN: 0331-8443
Electronic ISSN: 2467-8821
https://doi.org/10.67358/njt.2026.6319

MODELLING AND OPTIMISATION OF PROPERTIES OF HARDENED CALCINED CLAY-CALCIUM CARBIDE WASTE-BASED MORTAR USING RESPONSE SURFACE METHODOLOGY

AUTHORS:
*A. S. Oladimeji[1], M. A. Usman[1], E. E. Ikponmwosa[2] and R. U. Owolabi[1]

AFFILIATIONS:
[1]Department of Chemical and Petroleum Engineering, University of Lagos, Akoka, Yaba, NIGERIA
[2]Department of Civil and Environmental Engineering, University of Lagos, Akoka, Yaba, NIGERIA

***CORRESPONDING AUTHOR:**
Email: steveayodele20012001@yahoo.com

ARTICLE HISTORY:
Received: January 16, 2026.
Revised: April 28, 2026.
Accepted: May 09, 2026.
Published: June 17, 2026

KEYWORDS:
RSM, Modelling, Optimisation, Multivariable, Pozzolanic reaction

ARTICLE INCLUDES:
Peer review

DATA AVAILABILITY:
On request from author(s)

EDITORS:
Chidozie Charles Nnaji

FUNDING:
None

Abstract

The rise in demand for sustainable cementitious materials has driven interest in supplementary binders that use less Ordinary Portland Cement (OPC) without sacrificing performance. This study used a Central Composite Design-based Response Surface Methodology (RSM) to model and optimise the properties of hardened mortar containing calcined Ifonyintedo clay (CIC) and calcium carbide waste (CCW) as partial replacements for Portland Limestone Cement (CEM II), capturing the multivariable and interactive effects of hydration and pozzolanic reactions that are not addressed by conventional single-factor experimental methods. The influence of CEM II, CIC, and CCW contents, water–binder ratio, and curing age on compressive strength, density, and water absorption was systematically analysed, while thermogravimetric analysis (TGA), X-ray diffraction (XRD), and scanning electron microscopy (SEM) were used to characterise hydration products, phase assemblage, and microstructural evolution. Predictive models were developed and experimentally validated, with prediction errors below 5 %. Microstructural and phase analyses confirmed enhanced C–S–H formation and matrix densification at the optimum mix composition of 75.69 weight per cent (wt %) of CEM II, 19.13 wt % of CIC, and 5.20 wt % of CCW, at a water–binder ratio of 0.325. This optimum mix achieved a compressive strength of 39.1 MPa, a density of 2070 kg/m³, and a water absorption of 0.030 at 90 days. The results indicated that the partial replacement of CEMII with CIC–CCW can significantly reduce cement use while maintaining adequate mechanical and durability performance, thereby validating their viability as sustainable cementitious alternatives.

1.0 INTRODUCTION

Increasing environmental concerns about energy use and emissions of greenhouse gases from cement manufacturing have increased demand for sustainable construction materials, a challenge exacerbated by rapid global urbanisation, with the urban population anticipated to increase from 55 % in 2018 to approximately 68 % by 2050 [1, 2]. By 2050, emerging nations such as Nigeria may require up to 18 billion tons of concrete to build infrastructure [2, 3]. However, the manufacture of OPC produces about 0.8–0.9 t of CO_2 per ton of cement or around 8 % of the world's emissions. To meet growing worldwide construction demand, OPC production reached over 4.1 billion tons in 2020, allowing for the manufacture of roughly 25–30 billion tons of concrete [2, 4]. Interest in partially replacing OPC with supplementary cementitious materials (SCMs) such as calcined clay and natural pozzolans has increased due to the limited

HOW TO CITE:
Oladimeji, A. S., Usman, M. A., Ikponmwosa, E. E. and Owolabi, R. U. "Optimization Modeling Modelling and Optimisation of Properties of Hardened Calcined Clay-Calcium Carbide Waste-Based Mortar using Response Surface Methodology", *Nigerian Journal of Technology*, 2026. 45(2), pp. 307 - 319. https://doi.org/10.67358/njt.2026.6319

© 2026 by the author(s). This article is open access under the CC BY-NC-ND license

availability of fly ash, ground granulated blast furnace slag (GGBFS), as well as their economic and environmental benefits [3–5]. Calcined clay is a promising SCM due to its abundance, low calcination temperature, and capacity to improve mechanical and durability qualities, while alkali-rich calcium carbide waste (CCW) provides extra alkali for pozzolanic reaction, strengthening blended mortars even more.

However, careful optimisation of the mixing percentage is necessary to achieve the desired hardened properties, such as strength, density, and durability, to use both materials effectively [6–10]. Traditional trial-and-error mix design is laborious and inefficient, whereas Response Surface Methodology (RSM) allows effective analysis of variable interactions, predictive modelling, and mix proportions optimisation to enhance performance and sustainability [11, 12]. Kaolinite clays (≥34 weight per cent kaolinite) calcined at 600–850 °C exhibit high pozzolanic reactivity, making calcined clay a good alternative to typical SCMs, which are scarce [13]. While kaolinitic clays and clay-based blended systems have been the subject of several studies [14–16], the optimisation of calcined clay–OPC binders has mostly relied on trial-and-error methods, with statistical optimisation techniques being applied sparingly in cement and concrete research [11, 12, 17]. This study develops a pozzolanic binder by partially replacing OPC with CCW and calcined clay, using Central Composite Design-based RSM to optimise mix proportions, create predictive models, and encourage sustainable utilisation of CCW. RSM modelling shows that water–binder ratio, CIC and CCW contents, and curing duration all influence hardened mortar properties, with CIC supporting pozzolanic reactivity and C–S–H production, while CCW provides extra $Ca(OH)_2$, for pozzolanic reaction. Mineralogical and microstructural features are assessed using TGA, XRD, and SEM to measure hydration and pozzolanic activity. Statistical modelling, combined with experimental data, were employed to evaluate SCM synergistic effects and identify optimal mixture proportions for improved performance. This strategy supports sustainable construction by using industrial waste and abundant natural resources, thereby reducing cement use and its associated negative environmental impacts.

2.0 MATERIALS AND METHODS

2.1 Materials

CEM II/B-L 42.5 N Portland limestone cement from Dangote Cement Plc, which conforms to [18], was used for mortar production, with its chemical composition previously described [13]. Using Bogue's equations and according to the oxides composition in [13], the mineralogical phases were 61.7 weight per cent C_3S, 13.6 weight per cent C_2S, 7.3 weight per cent C_3A, and 8.4 weight per cent C_4AF. River sand from Abeokuta South, Ogun State, was used as fine aggregate; it complied with [19], passing the 2.00 mm screen and being kept on the 63 µm sieve, and was devoid of harmful materials. Unprocessed clay from Ifonyintedo, Ogun State (N 6° 32.674′, E 2° 51.305′), collected at 1 m depth, was calcined at an optimum temperature of 600 °C, as established in a prior study [13]. Calcium carbide waste (CCW), a by-product of acetylene production and environmental contaminant, was collected from roadside panel beaters in Ado-Odo/Ota. Before use, CCW and pulverised calcined clays were both sieved through a 75 µm mesh. The polycarboxylic ether-based superplasticiser, MasterGlenium Sky 504, supplied by Baden Aniline and Soda Factory (BASF), West Africa Limited, Lagos, Nigeria, and potable water conforming to [19] from the Covenant University Concrete Laboratory were used in the mixing process. Tables 1 and 2 present the physical properties of CEM II, CIC, and CCW, including specific gravity, specific surface area (SSA), Brauner Emmett and Teller (BET) surface area, and particle size distribution (PSD), as reported previously [13], consistent with [20].

Table 1: BET (SSA) and BJH mesoporous pore volume of the materials

Binder	BET SSA (m^2/g)		D_{90}	D_{50}	D_{10}	Pore diameter mode-DA (nm)	Pore Volume (cm^3/g)
	Single Point	MultiPoint					
CEMII	1.32×10^2	2.52×10^2	300	49.8	4.88	2.92	-
CCW	1.67×10^2	1.97×10^2	320	50	7.24	3.00	0.34
C-IF	0.81×10^2	1.37×10^2	743	353	3.6	3.00	0.14

© 2026 by the author(s). Licensee NIJOTECH.
This article is open access under the CC BY-NC-ND license.
https://doi.org/10.67358/njt.2026.6319
http://creativecommons.org/licenses/by-nc-nd/4.0/

Table 2:Materials physical properties

Properties	Sand	CEM II	CCW	CIC
Dry Density (kg/m^3)	1388.6	-	520.3	773.12
Bulk Density (kg/m^3)	1394.7	1255.3	647.6	893.50
Specific Gravity	2.61	3.12	2.31	2.71
Coefficient of Uniformity (Cu)	2.29	-	-	-
Curvature (Cc)	1.07	-	-	-
Moisture Content (%)	0.21	-	15.4	18.7
Fineness (passing through 90µm)	-	46.2	38	33.4

2.2 Methodology

2.2.1 Hardened mortar strength tests

Quantities of CEM II 42.5N Portland cement, fine aggregates, portable water, calcined clay, and calcium carbide waste were measured and used to prepare five 40x40x40 mm cubes of mortar per mix batch. Replicate reference sand [19], superplasticiser, and potable water were also applied as reported in our previous study [20]. Mixtures of mortars were produced as detailed in Table 3, with a mix ratio of 1:3 and a water/cement (w/c) ratio of 0.3, 0.35, and 0.4; selected by trial-and-error approach as water-cement ratios (w/c) in a binary mix of CEMII with CIC, as well as CEMII with CCW. The CEM II in the mix was partially replaced with calcined Ifonyintedo clay (CIC) at increments of 5 wt % ranging from 5 wt % to 30 wt % and CCW was also used to replace CEM II in a different mix at the same increment. The control mortar had a replacement of 0 % CCW and CIC. The mortar was mixed for about 4 minutes using a Hobart Corporation NSOLE 7-L pan mixer, tamped, and vibrated for 2 minutes with an Impart CN155 (1-ph, 60 Hz) vibrating table after it was put in moulds, to remove air voids. The moulds were covered to maintain controlled curing conditions, ensuring that variations in strength and hydration behaviour were attributable to the material composition and central composite Design (CCD) experimental factors rather than environmental fluctuations. Water bath curing was adopted, with specimens mixed and cast at 27 ± 2 °C and 75 ± 2 % RH, demoulded 24 h later, and cured at 22 ± 1 °C in water. Mortar cubes with a volume of 40 mm^3 were prepared using a 1:3 mix ratio at water–binder ratios of 0.30, 0.35, and 0.40. The binder composition was varied at 0, 5, 10, 15, 20, 25, and 30 wt %, resulting in 21 mix compositions (3 × 7). For each mix, five replicate cubes were tested at six curing ages: 3, 7, 21, 28, 90, and 120 days, yielding 30 cubes per mix (5 × 6) and a total of 630 cubes (21 × 30).

Figure 1: Mould utilised in this research

The prepared mortars cured for 3, 7, 21, 28, 90, and 120 days were subjected to tests on mortar strength and density. A 2000 kN LABTECH test machine was used for the compressive strength test as specified in [19].

Table 3: Mix ratio for mortar compressive strength

CEMII:CIC, CEMII: CCW	Water (g)	CEMII (g)	CIC /CCW (g)	Fine aggregate (g)	Superplasticiser (%)
Control	360, 420, 480	1200	-	3600	1
(5%)	360, 420, 480	1140	60	3600	1
(10%)	360, 420, 480	1080	120	3600	1
(15%)	360, 420, 480	1020	180	3600	1
(20%)	360, 420, 480	960	240	3600	1
(25%)	360, 420, 480	900	300	3600	1
(30%)	360, 420, 480	840	360	3600	1

© 2026 by the author(s). Licensee NIJOTECH.
This article is open access under the CC BY-NC-ND license.
https://doi.org/10.67358/njt.2026.6319
http://creativecommons.org/licenses/by-nc-nd/4.0/

2.2.2 Water absorption and density test on the hardened samples

The properties of the hardened mortar were assessed through water absorption and dry density measurements. in accordance with [21], water absorption was determined using 40 mm mortar cubes. The cubes were weighed after they were demolded to obtain the initial mass (m_1), submerged in water for the specified curing times, and reweighed to determine the wet mass (m_2). Equation (1) was used to compute water absorption.

$$WA = \frac{m_2 - m_1}{m_1} \quad (1)$$

2.2.3 Charcterisation of raw materials and hydration products

SEM (Phenom ProX) was used to examine binder morphology, XRD (Rigaku MiniFlex-600) to identify mineralogical phases, and TGA/DTA (PerkinElmer) to determine the degree of hydration, following procedures in [13]; all analyses were conducted at the Department of Chemical Engineering, Ahmadu Bello University, Zaria.

2.2.4 Design of the experiment

RSM-based optimisation was conducted using a CCD Design created using Design-Expert 10.0.3.0. Five process variables, CEM II, CIC, CCW contents, curing time, and water–binder ratio in Table 3, were investigated at 5 levels based on previous studies [8, 9]. These factors were varied to evaluate compressive strength, water absorption, and density as presented in Table 4.

The 46 experimental runs comprise 32 factorial points, 10 axial points, and 4 centre points; 3-5 centre points are sufficient for CCD involving five factors [8, 9, 17], as shown in equation 2.

$$N = 2^n + 2n + N_c \quad (2)$$

where N is the total number of experimental runs, n is the number of variables, 2^n is the factorial runs, and N_c is the number of centre-point replicates. A second-order polynomial was fitted to capture the main and interaction effects of the process variables according to equation 3. ANOVA with an F-test was used to evaluate factor significance and model adequacy, with terms having $p < 0.05$ considered significant and retained, while insignificant terms were removed to improve model reliability.

$$Y = \beta_0 + \sum_i^k \beta_i x_i \sum_i^k \beta_{ii} x_i^2 + \sum_i \sum_j \beta_{i,j} x_i x_j + \varepsilon_r \quad (3)$$

where xi and xj are independent variables at different levels, the predicted response is y, i and j span from 1 to the number of independent factors, the linear coefficient value is βi, the quadratic coefficient is βii, the interaction coefficient is βij, and the unique cause of variation or error is presented by εr. Calculated prediction error is given in equation 4; Y_{exp}, Y_{pred} are experimental and predicted responses.

$$Prediction\ error = \left|\frac{Y_{exp} - Y_{pred}}{Y_{pred}}\right| \times 100 \quad (4)$$

Multi-response optimisation using the desirability function method (DFM) maximised compressive strength, targeted density within a specified lightweight range, and minimised water absorption, with equally weighted responses combined through a geometric mean desirability index to identify the optimum mix.

Table 4: Variations in density, water absorption, and compressive strength based on central composite design

Variables	Units	Levels of coded variables				
		-α	-1	0	1	α
CEM II	g	393.50	490	560	630	726.51
CIC	g	85.62	35	122.5	210	330.62
CCW	g	10.87	35	52.5	70	94.11
H_2O	g	185.87	210	227.5	245	269.14
CT	days	11.36	30	60	90	131.37

2.2.5 Quantification of degree of hydration

The TGA curve was interpreted following [22] to determine the total degree of hydration at 3, 7, 28, and 120 days for the produced binder. Equations 5 and 6 were used to get the degree of hydration (α) and the chemically bound water (cbw).

$$cbw = 0.41(ldc) + ldh + ldx \quad (5)$$

$$\alpha = {cbw}/{0.24} \quad (6)$$

Ldh is the dehydration zone, representing mass loss from C–S–H breakdown; Ldx is the

© 2026 by the author(s). Licensee NIJOTECH.
This article is open access under the CC BY-NC-ND license.
https://doi.org/10.67358/njt.2026.6319
http://creativecommons.org/licenses/by-nc-nd/4.0/

dehydroxylationzone, showing mass loss from $Ca(OH)_2$ decomposition; and Ldc is the decarbonation zone, indicating mass loss from calcium carbonate decomposition.

3.0 RESULTS AND DISCUSSIONS

3.1 Influence of substituting a portion of CEMII with CIC at different water-binder ratios

From Figure 2(a-c), all mortar compressive strength decreased as the water/binder ratio (w/b) increased from 0.30 to 0.40, reflecting higher porosity and a less dense microstructure. At 0.30 w/b, both control and CIC-blended mixes achieve the highest strengths, with low to moderate CIC replacements (5–10wt %) approaching control values due to filler effects and early pozzolanic activity. At 0.35 w/b, the control shows superior early-age strength, while CIC replacements up to 10–15 % exhibit comparable later-age strengths from secondary C–S–H formation. At 0.40 w/b, overall strengths decline, and high CIC contents (≥20–30 %) further limit performance due to increased water demand and slower pozzolanic kinetics. Overall, partial replacement of CEM II with CIC is most effective at low to moderate replacement levels and lower w/b ratios, where densification and pozzolanic reactions offset cement dilution, with mortars meeting EN 197-1, and Class 32.5R standards [2, 5, 14, 23].

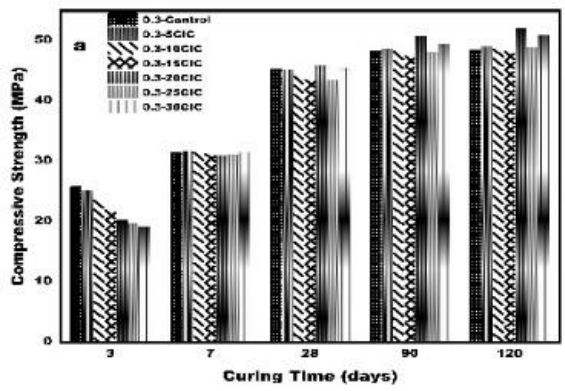

(a)

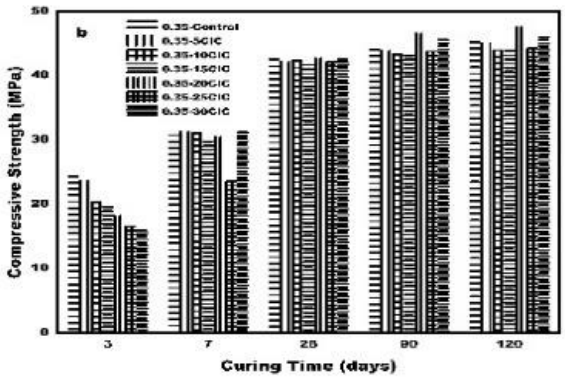

(b)

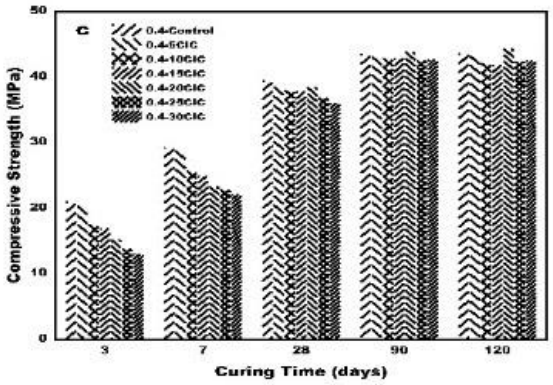

(c)

Figure 1: Strength of CEMII and CIC binary mix at water-binder ratios(a) 0.3 (b) 0.35 (c) 0.4

3.2 Mortar Strength of samples containing Calcium Carbide Waste

As shown in Figure 3(a & b), 5 wt % partial substitution of CEM II resulted to an average strength increase of about 0.6 MPa between 3 and 7 days of curing times at 0.3 and 0.35 water/binder ratios, respectively, as against the control, while no noticeable gain was observed at a 0.4 water/binder ratio in Figure 2c. This early-age improvement is attributed to the accelerating effect of CCW particles in forming C–S–H in addition to the growth in strength which resulted from the new hydration products like carboaluminate phases [24, 25]. In contrast, mortars with 10 wt % of CCW exhibited at least a 9.7% reduction in strength in all water/binder ratios, which [25] linked to CEM II saturation by CaO oxides from CCW. No appreciable increase in strength was noted between 28 and 120 days, confirming the non-pozzolanic nature of CCW; except for masonry applications, cement replacement levels above 10% CCW are unsuitable for structural concrete due to inadequate strength development.

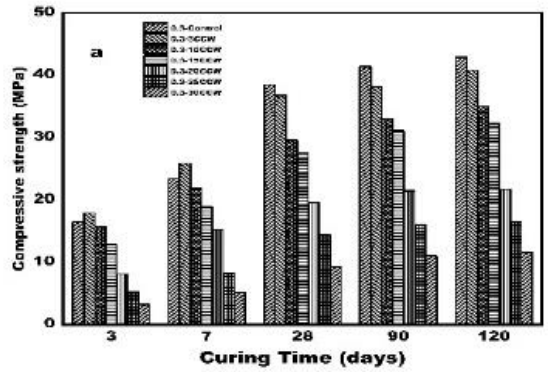

(a)

© 2026 by the author(s). Licensee NIJOTECH.
This article is open access under the CC BY-NC-ND license.
https://doi.org/10.67358/njt.2026.6319
http://creativecommons.org/licenses/by-nc-nd/4.0/

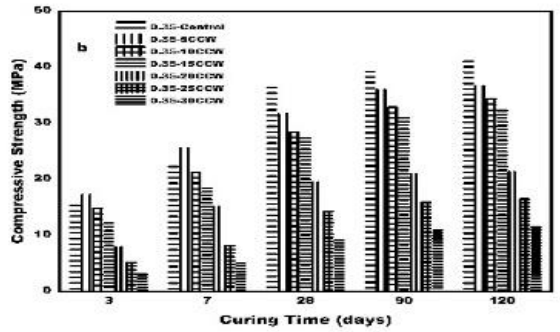

(b)

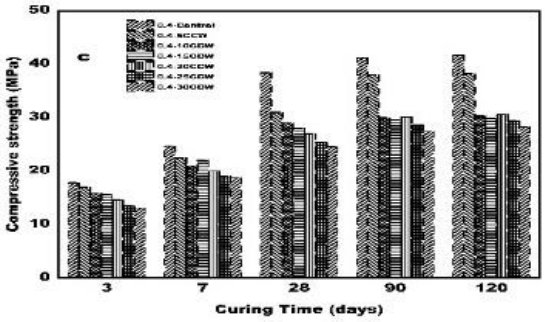

(c)

Figure 3: Strength of CEMII and CCW binary mix at water-binder ratios (a) 0.3 (b) 0.35 (c) 0.4

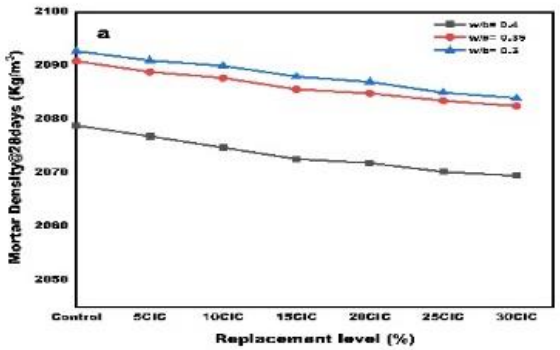

(a)

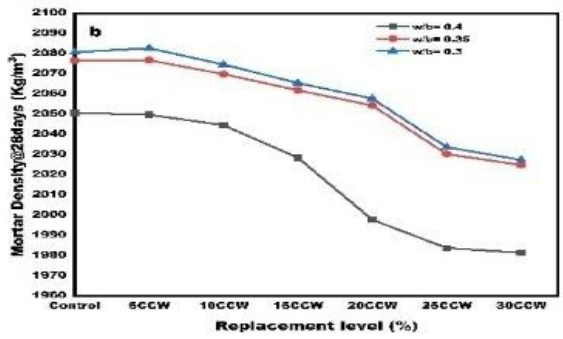

(b)

Figure 4: Density of CEMII binary mix with (a) CIC at w/b=0.3-0.4 (b) CCW at w/b= 0.3-0.4

3.3 Influence of Substitution of a Portion of CEMII with CIC and CCW on Density at Different Water/Binder Ratios

Figure 4a shows CEM II mortars reach maximum densities at the control level, with w/b = 0.30 yielding 2090–2095 kg/m³. Adding CIC gradually reduces density over period of 3–120 days, with minor losses at 10 % replacement (2075–2080 kg/m³, w/b = 0.30–0.35) and greater reductions at 20–30 % CIC (2050–2065 kg/m³), due to increased porosity and matrix dilution [5, 26]. Lower w/b ratios reliably increased density through improved particle packing [27, 28], while curing slightly raised or stabilised density as hydration and CIC pozzolanic activity densified the microstructure [28, 29]. At higher CIC and w/b ratios, density remains low across all ages due to slower reactions and increased porosity [28]. From Figure 4(b), the 28-day density results show a clear reduction with increasing CCW replacement of CEM II across all water–binder (w/b) ratios. Control mixes had densities of ~2050 kg/m³ (w/b = 0.40) and 2075–2080 kg/m³ (w/b = 0.30–0.35); 10 % CCW modestly decreased density to 2040–2060 kg/m³, while 20–30 % CCW caused significant drops to 1980–2030 kg/m³, lowest at w/b = 0.40. Lower w/b ratios (0.30–0.35) maintained higher densities across all CCW levels, reflecting improved particle packing and matrix compactness, as reported previously for low-reactivity cement replacements [30, 31]. The lack of density recovery at 28 days suggests limited late-age densification, in line with [32], which notes that calcium-rich industrial wastes with low pozzolanic activity minimally modify the CEM II matrix at early ages.

3.4 Water Absorption for CIC and CCW Mortar

From Figure 5(a–b), the water absorption of CEM II mortars increases with both CIC and CCW replacement levels and with increasing water–binder (w/b) ratio. At 28 days, the control mixes exhibited the lowest absorption values (0.04–0.06 for w/b = 0.30–0.35 and about 0.08 for w/b = 0.40). Low replacement levels (5–10 %) resulted in only marginal increases in absorption, whereas higher replacements (20–30 %) led to a pronounced rise (0.07–0.12), reflecting increased porosity and pore connectivity, as similarly reported by [3, 6, 33]. In line with durability trends observed for blended cement and SCM systems by [16], such changes may negatively impact durability if not addressed through lower w/b ratios. Water absorption remained high (≥20 %) at higher replacement levels, showing limited late-age densification, but declined slightly after 28 days at low replacement levels due to partial pore refinement. Lower water/binder ratios

© 2026 by the author(s). Licensee NIJOTECH.
This article is open access under the CC BY-NC-ND license.
https://doi.org/10.67358/njt.2026.6319
http://creativecommons.org/licenses/by-nc-nd/4.0/

consistently reduced absorption, reflecting improved matrix compactness and pore structure.

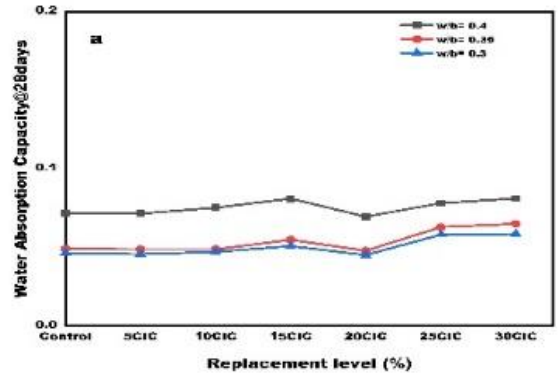

(a)

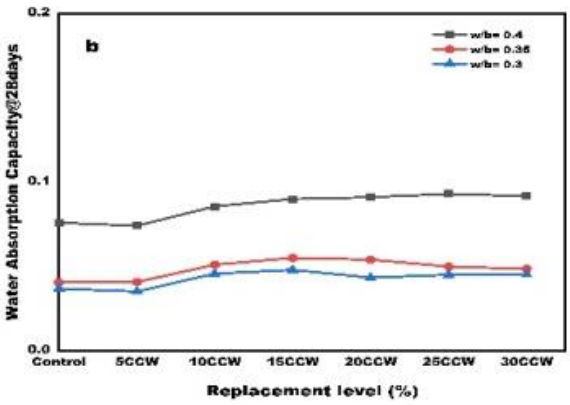

(b)

Figure 5: Water absorption in a binary combination of CEMII with CIC and CCW at water/binder ratios (a) 0.3-0.4 (b) 0.3-0.4

3.5 Regression Model Equations for HardenedMortar

Table 5 shows that models for water absorption, density, and compressive strength are highly reliable, with $R^2 > 97\%$, adjusted $R^2 \approx 96\%$, predicted $R^2 > 91\%$, and insignificant lack-of-fit, in line with recent blended cement optimisation studies [11, 12, 17]. Compressive strength is positively influenced by CEM II and curing time, as indicated by linear coefficients of +1.11 and +0.96 respectively, while excessive cement ($-1.82A^2$), calcined clay ($-3.60B$ and $-6.91B^2$), and higher water–binder ratio ($-2.06D$) significantly reduce strength due to dilution, slower pozzolanic kinetics, and increased porosity, in agreement with findings reported between [8, 11, 12, 17]. High calcined clay replacement decreased strength, whereas moderate CCW content ($+2.07\,C^2$) contributed positively, boosting strength via $Ca(OH)_2$ supply and improved pozzolanic reactivity, consistent with recent waste-derived binder studies [6, 13, 34]. Density decreases with calcined clay (-22.88 B), CCW (-12.97 C), and water (-28.65 D), but rises with cement ($+16.87$ A) and extended curing ($+29.08\,E^2$), underscoring the significance of water control and optimal filler effects for densification. Water absorption rises with calcined clay, CCW, and water–binder ratio, but falls with higher cement content (-3.52×10^{-3} A) and extended curing ($-0.010\,E^2$), supporting recent findings [34] that long-term curing, low water demand, and balanced binder composition are essential for durable, low-permeability mortars.

Table 5: The quadratic models with respect to the variables' coded values

Response	Regression Equation	R^2 (%)	Pred. R^2(%)	Adj R^2(%)	Lack of fit
(CS) Compressive Strength	38.81+1.11A-3.60B-0.81C-2.06D+0.96E+0.61AB-1.32AC-0.91AD-0.62AE+0.09BC-0.17BD+0.52BE-0.22CD+0.51CE-0.47DE-1.82A^2-6.91B^2+2.07C^2-1.04D^2+3.43E^2	97.88	92.28	96.19	1.60
(D) Density	2076.95+16.87A-22.88B-12.97C-28.65D+0.24E+5.97AB-17.86AC-1.86AD-11.12AE+6.67BC-4.48BD-8.07BE+8.84CD+5.62CE-2.18DE-75.46A^2-98.97B^2+37.07C^2+29.56D^2+29.08E^2	97.83	92.83	96.09	0.71
(WA) Water Absorption Capacity	0.017--3.516E-003A+6.102E-003B+5.268E-003C+6.963E-003D+2.715E-004E-9.973E-003AB+6.162E-003AC+1.636E-003AD-6.465E-004AE-6.922E-004BC+4.254E-004BD-1.232E-003BE+5.193E-003CD-1.827E-003CE+4.152E-003DE+0.013A^2+1.573E-003B^2+3.387E-003C^2+0.012D^2-0.010E^2	97.78	91.68	96.00	6.72

A= CEM II, B = CIC, C = CCW, D = H_2O, E = Curing time (CT)

© 2026 by the author(s). Licensee NIJOTECH.
This article is open access under the CC BY-NC-ND license.
https://doi.org/10.67358/njt.2026.6319
http://creativecommons.org/licenses/by-nc-nd/4.0/

3.5.1 Analysis of response surface

Compressive strength depends on the interaction of CCW and CIC contents, ranging from 28 to 45 MPa based on mix proportions, curing time, and water/binder ratio, as illustrated in the 3D response surface in Figure 6a. Improved packing density and increased hydration lead to higher strengths (38–45 MPa) at low water–binder ratios (≤0.35) with moderate CCW (100–150 g) and CIC (120–180 g) [16, 33, 34]. Strength drops to roughly 30–34 MPa at larger water–binder ratios (up to 0.4) and greater replacement levels because of increased porosity and cement dilution [6, 17, 34]. An ideal interaction zone is identified by the surface curvature, where balanced CCW–CIC proportions offer pozzolanic reactivity and synergistic lime supply, densifying the matrix and enhancing late-age performance [28, 29, 34]. The findings thus verify that while excessive incorporation at high w/b ratios degrades the microstructure, optimised CCW–CIC dose combined with low water–binder ratios increases compressive strength with curing time.

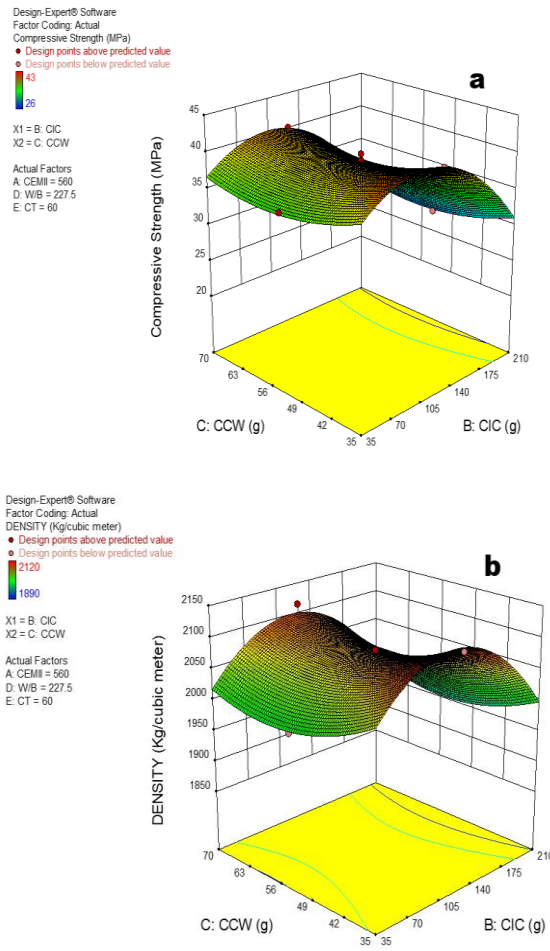

Figure 6: CCW and CIC interaction in (a) compressive strength, (b) density

According to Figure 6b's 3D response surface, the density of hardened mortar ranges from roughly 1849 to 2152 kg/m³, and it increased dramatically as the Calcined Ifonyintedo Clay (CIC) proportion increased from 35 to 210 g, due to its potent densifying and pozzolanic actions. Compared with cement or CIC, increasing the calcium carbide waste (CCW) proportion from 35 to 70 g typically decreases density, suggesting either increased porosity or weaker matrix compaction. High CIC and low CCW contents result in maximum densities, whereas low CIC and high CCW levels show minimum values, indicating decreased compactness.

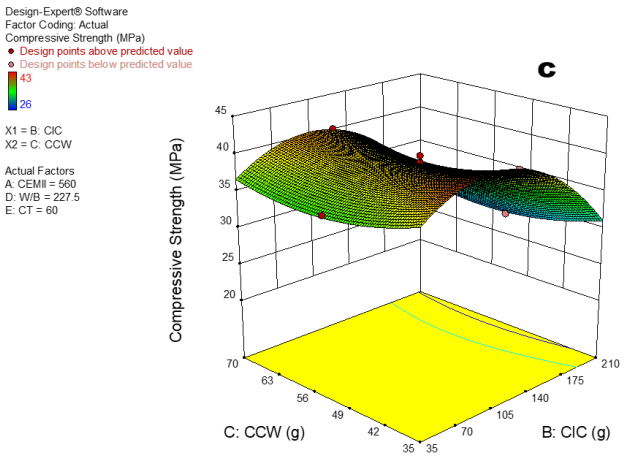

Figure 6: CCW and CIC interaction in (c) water absorption

The surface slope indicates that the positive impact of CIC on density outweighs the negative impact of CCW. Consistent with previous studies [6, 28, 29], optimising CIC is essential to prevent density loss from CCW when cement (560 g), water/binder ratio (227.5 g), and 60-day curing are constant. Increasing CIC from 35 to 210 g reduces water absorption to 0.01–0.02% at 105–140 g, as shown in Figure 6c. Absorption slightly climbs beyond the ideal CIC range, suggesting excess may remain unreacted or act as filler [29, 32], while increasing CCW from 35 to 70 g regularly increases water absorption by 0.01–0.07% because of its lightweight, irregular, and less reactive particles [34]. The most absorption is seen at high CCW (70 g), and low CIC (35 g), indicating inadequate pore refinement and increased permeability [4, 34]. The lowest absorption is found at low CCW (35 g) with moderate CIC (105–140 g). Optimising CIC dose is key to reducing CCW's negative effect on permeability and supporting durable blended mortars, even with 560 g cement, 227.5 g water/binder ratio, and 60-day curing [16, 17].

© 2026 by the author(s). Licensee NIJOTECH.
This article is open access under the CC BY-NC-ND license.
https://doi.org/10.67358/njt.2026.6319
http://creativecommons.org/licenses/by-nc-nd/4.0/

.3.5.2 Optimisation and validation

An ideal binder density of 2107 kg/m³, a compressive strength of 41.10 MPa, and a water absorption of 0.029 after 90 days was optimised. Strong agreement with model predictions was indicated by average values of 39.1 MPa compressive strength (maximised; 4.85 % error), 2070 kg/m³ density (Targeted; 1.71% error), and 0.030 water absorption (minimised; 3.44 % error) obtained from validation testing (triplicate), with a desirability of 1.000. According to results on calcined clay–cement systems, the blended cement showed densities ranging from 1920 to 2070 kg/m³, with greater values at ideal conditions due to post-28-day matrix densification [16]. Water absorption increased up to 28 days, then decreased and stabilised by 90–120 days due to pozzolanic pore refinement. Experimental and predicted results closely matched, validating the optimisation model, while 28-day compressive strengths of 86.5–99.5% of CEM II met the requirements in [35, 36], demonstrating the technical viability and sustainability of the CIC–CCW ternary blend.

3.6 Characterisation

3.6.1 SEM analysis

At 90 days, the hydrated CEM II microstructure (Figure 7a) is characterised by a dominant C–S–H gel with visible CH and AFm phases, residual C–S and C_2S, and a relatively porous interfacial transition zone (ITZ), indicating limited late-age densification typical of plain Portland cement systems [16, 37, 38]. In contrast, the blended cement sample with added 20 wt % CIC (Figure 7b) shows a markedly denser and more homogeneous matrix, with increased secondary formation C–S–H caused by pozzolanic reactions and a refined ITZ containing fewer large CH crystals, consistent with recent findings on SCM-modified binders [37, 38]. Regression results indicated that longer curing improves strength and less water absorption due to better particle packing and lower porosity in the blended system. With a well integrated ITZ, expanded C–S–H, and significant CH consumption, the ternary binder with optimal parameters (Figure 7c) has the most compact microstructure, demonstrating that more calcium speeds up and maintains pozzolanic processes [37]. Microstructural analysis of the three systems supports literature trends
[37], showing improved late age hydration, ITZ quali ty, and durability.

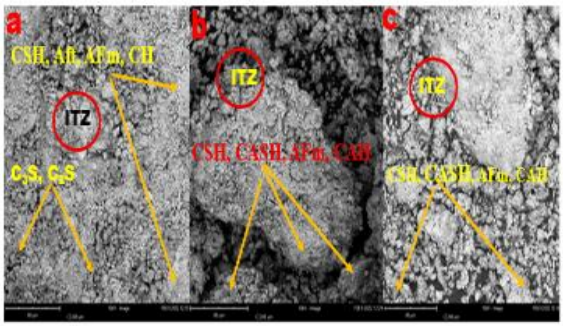

Figure 7: Microstructure change after 90 days for (a) hydrated CEM II, (b) a combined cement sample containing 20 % CIC, and (c) ternary blended cement.

3.6.2 X-ray diffraction

Given the XRD patterns shown in Figure 8, the reference cement (CEM II) exhibits early-age Ettringite development and sustained Portlandite formation across all curing ages, suggesting ordinary hydration with few secondary reactions [38, 39]. Between 7 and 90 days, blended cement pastes exhibit decreasing Portlandite intensity, indicative of pozzolanic consumption of $Ca(OH)_2$ and production of extra C–S–H, which improves later-age strength [38]. Stabilisation or partial transformation of ettringite and the appearance of monocarboaluminate phases indicate increased carbonate–aluminate interactions, which enable better dimensional stability and sulfate resistance [39]. Increased calcite in blended systems encourages microstructural densification through filler and nucleation effects, reducing pore connectivity and enhancing durability, including permeability [40]. Blended cements exhibit better long-term strength and durability compared to CEM II due to reduced Portlandite and the production of stable carbonate–aluminate phases [39]. Figure 8 displays the XRD trace of the reference and blended cement pastes that were cured for seven, thirty, and ninety days.

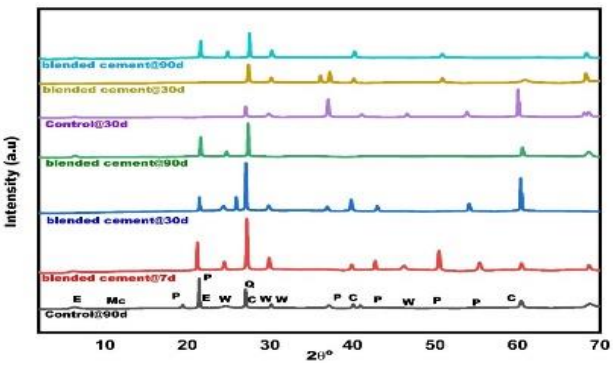

Figure 8: P: Portlandite ($Ca(OH)_2$), C: Calcite,W Wollastonite, Q: Quartz, Mc:Monocarboaluminat e, and E: Ettringite

© 2026 by the author(s). Licensee NIJOTECH.
This article is open access under the CC BY-NC-ND license.
https://doi.org/10.67358/njt.2026.6319
http://creativecommons.org/licenses/by-nc-nd/4.0/

3.6.3 Degree of hydration of the ternary binder

Figure 9 shows three TGA mass-loss regions for control, CIC, and CIC-CCW blended cements after 90 days, with the 100–300 °C range showing higher mass loss in the blended systems than in the control, indicating increased bound water and C–S–H production [40]. According to studies by [41], the blended systems, especially the 20 weight per cent CIC mix, show lower CH, confirming enhanced pozzolanic activity, while the control shows increased mass loss in the 400–500 °C range due to a higher portlandite (CH) concentration. There are only slight variations between the mixes in the 600–800 °C range, with blended cements typically having lower carbonate concentrations caused by material and CCD factors. Therefore, the evolution from 90 to 120 days confirms the presence of continuous pozzolanic reactions and enhanced microstructural development in the blended systems, as evidenced by increased hydration and maintained CH consumption. Table 6 summarises the relevant weight-loss statistics.

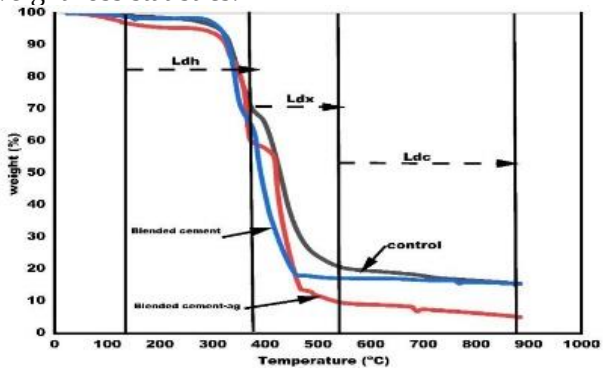

Figure 9: Loss of weight % vs temperature

Table 6: TGA loss in weight for cement-calcined clay and calcium carbide

Curing Age (Days)		Weight Loss			Degree of Hydration (%)
		Ldh	Ldx	Ldc	
CEMII	3	12.2	2.6	2.0	62
	7	12.7	3.4	3.1	68.3
	28	12.8	3.8	3.3	74.2
	120	14.0	4.5	3.5	76.6
CEMII20CIC	3	11.4	1.7	3.2	55
	7	11.8	2.4	3.1	60
	28	14.1	2.6	3.3	74.5
	120	14.5	2.7	3.3	78.6
OPTIMUM	3	11.7	1.9	3.1	58.2
	7	12.3	2.5	3.2	63
	28	13.5	2.7	3.3	75
	120	14.1	2.9	3.4	78.4

3.7 Influence of Calcined IfonyintedoClay and Calcium Carbide Waste on Hydration of the Mortar

In line with earlier research on blended cement systems [40], the TGA data in Table 6 show gradual mass loss with curing age across all systems, indicating ongoing hydration and increased production of chemically bound water and hydrates. For CEM II, the degree of hydration improves from 62 % to 76.6 %, indicating consistent continuous hydration, but the overall mass loss increases from roughly 12.2 % at 3 days to 14.0 % at 120 days. Early-age hydration is reduced in the CEM II–20% CIC blend (55–60 % over 7 days). However, due to delayed but accelerated pozzolanic reactions of calcined clay, it surpasses CEM II at later ages, reaching 78.6 % at 120 days, as also observed by [40]. The optimal ternary CEM II–CIC–CCW combination exhibits moderate early-age hydration (58–63 %) but attains equivalent late-age hydration (78.4 % at 120 days), highlighting the complementary roles of CIC as a pozzolanic material and CCW as a lime source. Increasing contributions of Ldh, Ldx, and Ldc with curing age reflect progressive production of C–S–H and other hydrates, explained the improved strength and densification at later ages.

4.0 CONCLUSION

This study successfully applied Response Surface Methodology to model and optimise the hardened properties of calcined clay–calcium carbide waste (CIC–CCW) blended mortar, with validated second-order models showing strong predictive accuracy for water absorption, density, and compressive strength. The optimised mix achieved a compressive strength of 39.1 MPa, a density of 2070 kg/m³, and a water absorption of 0.030 with a desirability of 1.000, showing close agreement between predicted and measured values. These findings demonstrate how

© 2026 by the author(s). Licensee NIJOTECH.
This article is open access under the CC BY-NC-ND license.
https://doi.org/10.67358/njt.2026.6319
http://creativecommons.org/licenses/by-nc-nd/4.0/

CCW's lime-bearing properties and CIC pozzolanic reactivity work together to improve matrix densification and durability. Microstructural and thermal characterisation (SEM, XRD, and TGA) further confirmed that the optimised blend developed well-formed hydration products, reduced porosity, which validates its suitability as a sustainable cementitious binder.

REFERENCES

[1] United Nations Department of Economic and Social Affairs. *68% of the World Population Projected to Live in Urban Areas by 2050*. United Nations, New York, NY, USA, 16 May 2018. Available online: https://www.un.org/development/desa/en/news/population/2018-revision-of-world-urbanization-prospects.html

[2] Akindahunsi, A. A., Avet, F., and Scrivener, K. "The Influence of some calcined clays from Nigeria as clinker substitute in cementitious systems," *Case Studies in Construction Materials*, 13, p. e00443, 2020. doi: https://doi.org/10.1016/j.cscm.2020.e00443.

[3] Arum, R. C., Arum, R., and Alabi, S. A. "The highs and lows of incorporating pozzolans into concrete and mortar: A review on strength and durability," *Nigerian Journal of Technology*, 41(2), pp. 197–211, 2022. http://dx.doi.org/10.4314/njt.v41i2.1

[4] Rubayat, K. M., Bediwy, A., Kanaan, D., Alam, M. S., and Hossain, K. M. A. "Valorisation of partially combusted wood fly ash with nano-silica as low-impact alternative to coal fly ash in cementitious composites," *Journal of Clean Production*, 538, pp. 147-151, 2026. https://doi.org/10.1016/j.jclepro.2026.147251

[5] Scrivener, K., Martirena, F., Bishnoi, S., and Maity, S. "Calcined clay limestone cements (LC3)," *Cement and Concrete Research, 114*, pp. 49–56, 2018. https://doi.org/10.1016/j.cemconres.2017.08.017

[6] Adamu, M., Olutoye, M. A., Eterigho, E. J., and Yahya, M. D. "Response Surface Methodology (RSM) optimisation and characterisation of silica production from Bida rice husk," in *Proceedings of Academic Conference, Mediterranean Resources, Publication, International*, Usmanu Danfodiyo Univ., Sokoto, 7, pp. 33-38, 2025. https://doi.org/10.70383/mejnsar.v7i9.030

[7] Teong, S. P., and Zhang, Y. "Calcium carbide and its recent advances in biomass conversion," *Journal of Bioresources and Bioproducts*, 5(2), pp. 96-100, 2020. https://doi.org/10.1016/j.jabab.2020.03.001

[8] Adedokun, S. I., Oluremi, J. R., Mark, D. O., Anifowose, M. A., and Lawal, A. R. "Effects of substitution of cement with ground granulated slag on concrete," *Nigerian Journal of Technology*, 43(3), pp. 400–410, 2024. https://doi.org/10.4314/njt.v43i3.1

[9] Ogunro, A. S., Usman M. A., Ikponmwosa, E. E., and Owolabi, R. U. "Optimisation and modeling of fresh state properties of cement-calcined clay-calcium carbide waste pastes using the RSM," *Advances in Cement and Concrete Materials Research*, 51, pp.118-127, 2025. https://doi.org/10.21741/9781644903537-14

[10] Ikponmwosa, E. E., Olonade, Sulaiman, A. O., Akintunde, E. O., Enikanolog, N. O., and Kehinde, O. A. "Mix design optimisation of high-performance concrete using local materials." *Nigerian Journal of Technology*, 42(2), pp. 167 – 174, 2023. https://doi.org/10.4314/njt.v42i

[11] Li, Z., Lu, D., Gao, X. "Optimisation of mixture proportions by statistical experimental design using response surface method," *Journal of Building Engineering*, 36, p. 101, 2021. https://doi.org/10.1016/j.jobe.2020.101617.

[12] Lin, R.-S., Han, Y., Wang, X. Y. "Experimental study on optimum proportioning of Portland cements, limestone, metakaolin, and fly ash for obtaining quaternary cementitious composites," *Case Studies in Construction. Materials*, 15, p. e00691 2021. doi: 10.1016/j.cscm.2021.e00691.

[13] Ogunro, A. S., Usman M. A., Ikponmwosa, E. E., and Owolabi, R. U. "Applicability of calcined clay and CCW in cement mixes for development of pozzolanic binder," *Nigerian Journal of Technology*, 44(1), p.411420, 2025. https://doi.org/10.4314/njt.v44i1.1

[14] Zhou, D., Wang, R., Tyrer, M., Wong, H., and Cheeseman, C. "Sustainable infrastructure development through the use of calcined excavated waste clay," *Journal of Cleaner Production*, vol. 168, pp. 11801192, 2017. doi: https://doi.org/10.1016/j.jclepro.201 7.09.098.

[15] Jaskulski, R., JóźwiakNiedźwiedzka, D. and Yakymechko, Y., "Calcined Clay as supplementary cementitious material," *Materials*, 13(21), p. 4734, 2020. doi: 10.3390/ma13214734

© 2026 by the author(s). Licensee NIJOTECH.
This article is open access under the CC BY-NC-ND license.
https://doi.org/10.67358/njt.2026.6319
http://creativecommons.org/licenses/by-nc-nd/4.0/

[16] Islam, M. S., Kar, P., Maleque, M. S. E., and Mohr, B. J. "Properties of calcined clay blended ASTM Type IL cementitious materials," *Next Materials*, 9, p. 101053, 2025. https://doi.org/10.1016/j.nxmate.2025.101053

[17] Quiatchon, P. R. J., Dollente, I. J. R., Abulencia, A. B., Libre Jr, R. G. D. G., Villoria, M. B. D., Guades, E. J., Promentilla, M. A. B., and Ongpeng, J. M. C. "Investigation on the compressive strength and time of setting of low-calcium fly ash geopolymer paste using response surface methodology," *Polymers*, 13(20), p. 3461, 2021. https://doi.org/10.3390/polym13203461

[18] BS EN 197. *Cement Part 1: Composition, Specifications, and Conformity Criteria for Common Cements*, 2011

[19] BS EN 196. *Methods of testing cement - Part 1: Determination of strength*. London, 2016.

[20] Ikponmwosa, E., Fapohunda, C., and Ehikhuenmen, S. "Suitability of Polyvinyl Waste Powder as Partial Replacement for Cement in Concrete Production," *Nigerian Journal of Technology*, 33(4), pp. 504, 2014, doi: https://doi.org/10.4314/njt.v33 i4.11.

[21] European Committee for Standardization, *EN 1008: Methods of Test for Water for Making Concrete*, British Standards Institution, London, U.K., 2002.

[22] ASTM C830-00, *Standard Test Methods for Apparent Porosity, Liquid Absorption, Apparent Specific Gravity, and Bulk Density of Refractory Shapes by Vacuum Pressure*, ASTM International, West Conshohocken, PA, USA, 2016.

[23] Bhatty, J. I. "Hydration versus strength in a Portland cement developed from domestic mineral waste-A comparative study," *ThermochimicaActa*, 106, pp. 93-103, 1986. https://doi.org/10.1016/0040-6031(86)80020-2

[24] Zunino, F., Haha, M. B., Skibsted, J., Joseph, S., Krishnan, S., Parashar, A., and Juenger, M. "Hydration and mixture design of calcined clay blended cement: review by the RILEM TC 282-CCL," 55(9), 2022. doi: https://doi.org/10.1617/s11527022-02060-1.

[25] Gora, A. M., Ogork, E. N., and Haruna, S. I. "Effect of CCW as an admixture in mortar," *Scholars Journal of Engineering and Technology*, *5*(11), pp. 655–660, 2017. https://doi.org/10.21276/sjet.2017.5.11.6

[26] Kabilis D. M., Ejike, I. K., Amartey, Y. D., Lawan, A., and Nyela, J. Y. "Laboratory Experiment on the Effect of CCW and Metakaolin on Strength and Durability Properties of Blended Concrete," *Covenant Journal of Engineering Technology*, 6, pp. 12-20, 2023. https://journals.covenantuniversity.edu.ng/index.php/cjet/article/view/3798

[27] Hollanders, S., Adriaens, R., Skibsted, J., Cizer, O., and Elsen, J. "Pozzolanic reactivity of pure calcined clays. *Applied Clay Science* 133, pp. 552–560, 2016. https://doi.org/10.1016/j.clay.2016.08.003

[28] Juenger, M.C., Snellings, R., and Bernal, S.A "SCMs: New sources, characterisation, and performance insights," *Cement and Concrete Research*, 122, pp. 257–273, 2019. https://doi.org//10.1016/j.cemconres.2019.05.008

[29] Zhou, D. "*Developing Supplementary Cementitious Materials from Waste London Clay*," PhD dissertation, Imperial College London, London, U.K., 2016.

[30] Zayed, A., Shanahan, N., Sedaghat, A., Stetsko, Y., and Lorentz, B."Development of calcined clays as pozzolanic additions in portla nd cement concrete mixtures,"*University of So uth Florida, Department of Civil and Environ mental Engineering*, Tampa, FL, USA: Department of Civil and Environmental Engineering, University of South Florida, pp.4551, 2018. https://doi.org/10.1190/usfd.2018.25977

[31] Provis, J. L. "Alkali-activation of calcined clays–past, present and future. In: Calcined clays for sustainable concrete," *Springer*, pp. 372–376, 2018.

[32] Kosar, H., Yasemin, A., Mehmet Can, D., OwYang, C. W., and Ali Gulgun, M. "Effect of metakaolin and lime on strength development of blended cement paste," *Construction materials*, 2(4), pp.297-313, 2022. doi: https://doi.org/10.3390/constrmater2040019.

[33] Wang, Q., Wang, Y., Gu, X., Liu, J., and Xu, X. "Study on the properties and hydration mechanism of calcium carbide residue-based low-carbon cementitious materials," *Buildings*, 14(5), pp. 1259, 2024. https://doi.org/10.3390/buildings14051259

[34] Pantić, V., Šupić, S., Vučinić-Vasić, M., Nemeš, T., Malešev, M., Lukić, I., and Radonjanin, V. "Effects of grinding methods and water-to-binder ratio on the properties of cement mortars blended with bio-ceramic powder," *Materials*, *16*(6), p. 2443, 2023. https://doi.org/10.3390/ma16062443

[35] Bawab, J., El-Hassan, H., El-Dieb, A., Khatib, J., and El-Mir, A. "Utilisation of calcium

© 2026 by the author(s). Licensee NIJOTECH.
This article is open access under the CC BY-NC-ND license.
https://doi.org/10.67358/njt.2026.6319
http://creativecommons.org/licenses/by-nc-nd/4.0/

carbide residue as a concrete component: A comprehensive review," *Case Studies in Construction Materials*, 22(e04823), 2025. doi: 10.1016/j.cscm.2025.e04823.

[36] Nigeria Industrial Standard, *Cement, Composition, specifications and conformity criteria for common cements*, NIS 444-1:2018, Standards Organisation of Nigeria, 2018.

[37] ASTM C618. *Specifications for Coal Fly Ash and Raw or Calcined Natural Pozzolan for Use in Concrete*, ASTMs, West Conshohocken; 2022.

[38] Sui, H., Hou, P., Liu, Y., Sagoe-Crentsil, K., Basquiroto de Souza, F., and Duan, W. "Limestone Calcined Clay Cement: Mechanical Properties, Crystallography, and Microstructure Development," *Journal of Sustainable Cement-Based Materials*, 12, pp.1–14, 2022. https://doi.org/10.1080/21650373.2022.2059717

[39] Zarzuela Sánchez, R., Luna Aguilera, M. J., Martínez Carrascosa, L. A., Yeste Siguenza, M. D. P., Garcia-Lodeiro, I., Blanco-Varela, M. T., Mosquera Díaz, M. J. "Producing C-S-H gel by reaction between silica oligomers and portlandite," *Cement and Concrete Research*, 130, pp. 106008–106008, 2020. doi: https://doi.org/10.1016/j.cemconres.2020.106008.

[40] Alujas, A., Fernández, R., Quintana, R., Scrivener, K. L., and Martirena, F. "Pozzolanic reactivity of low-grade kaolinitic clays: Influence of calcination temperature and impact of calcination products on OPC hydration," *Applied Clay Science*, 108, pp. 94–101, 2015. doi: https://doi.org/10.1016/j.clay.2015.01.028.

[41] Ojaruega, A. M. "Hydration of Binary and Tertiary Fly Ash and Quicklime Blended Cement Paste System," *M.Sc. thesis, Univ. of North Carolina at Charlotte, Charlotte, NC, USA*, pp. 145-150 2018.

© 2026 by the author(s). Licensee NIJOTECH.
This article is open access under the CC BY-NC-ND license.
https://doi.org/10.67358/njt.2026.6319
http://creativecommons.org/licenses/by-nc-nd/4.0/